Ultra-slow ammonia flame speeds - A microgravity study on radiation

Roman Glaznev, Christian Schwenzer, Raik Hesse, Sanket Girhe, Fabien Halter, Christian Chauveau, Heinz Pitsch, Joachim Beeckmann

Proceedings of the Combustion Institute 40 (2024) 105334

Contents lists available at ScienceDirect

Proceedings of the Combustion Institute

journal homepage: www.elsevier.com/locate/proci

Ultra-slow ammonia flame speeds — A microgravity study on radiation

Roman Glaznev [a,*], Christian Schwenzer [a], Raik Hesse [a], Sanket Girhe [a], Fabien Halter [b,c], Christian Chauveau [b], Heinz Pitsch [a], Joachim Beeckmann [a]

[a] Institute for Combustion Technology, RWTH Aachen University, 52056 Aachen, Germany
[b] CNRS-INSIS, ICARE, 45071 Orléans, France
[c] Université d'Orléans, 45100 Orléans, France

ARTICLE INFO

Keywords:
Ammonia
Radiation
Microgravity
Laminar flame speed
Flame propagation

ABSTRACT

Ammonia/air flames burn slowly and are consequently affected by buoyancy-, radiation-, and stretch-related uncertainties more than many conventional hydrocarbon fuels. In this work, unique buoyancy-free ammonia/air flame speed data were acquired and analyzed, specifically considering the impact of radiation. First, outwardly propagating ammonia/air flames near the propagation limits were accurately measured under microgravity using two simultaneous techniques. Flame radius evolution was captured by a high-speed Schlieren arrangement (optical method) in a near-isobaric regime. Accompanying, pressure rise was measured and subsequently used for flame speed extraction during near-isentropic gas compression. A profound nonlinear dependence of flame propagation speed on stretch was captured over the optical results in the observable range of the current setup, which illustrates the limitations of the optical method in comparison to the pressure-rise method. Radiation-corrected optical and pressure-rise results have shown good agreement along multiple isentropes, thereby cross-validating applied methodologies and highlighting very good consistency of the acquired data. Pressure-rise data analysis has shown sensitivity in the assessment of kinetic mechanisms to the radiation effect. In the absence of appropriate radiation correction for flame speed data, misinterpretations may arise regarding the accuracy of kinetic models, introducing challenges in the development of accurate kinetic models. The performance of the chemical kinetic models was quantified in a wide range of unburned gas temperatures (< 500 K) and pressures (< 9.3 bar) against distinctive experimental flame speed data with and without radiation correction acquired under microgravity indicating good performance of the Han et al. (2019) model.

1. Introduction

Energy production from renewable sources, such as wind, solar, and water is typically intermittent and location-bound. Thus, energy storage and transportation are unavoidable necessities. Using chemical energy carriers such as ammonia is one option that is lately considered for this purpose [1]. Stored ammonia can be burned in combustion devices to recover the energy without CO_2 emissions [2]. However, ammonia is characterized by low reactivity, slow flame propagation, NH_3 slip (unreacted ammonia emissions), and potentially high NO_x emissions, yielding challenges for applications such as burners or engines [1]. The dynamics of ammonia flames must be well understood to design suitable combustion technologies. Hence, accurate experimental data on the fundamental combustion properties of ammonia, such as the laminar flame speed ($S^0_{L,u}$), are required.

The outwardly propagating flame (OPF) technique has gained widespread use for measuring $S^0_{L,u}$ of non-buoyant flames, owing to the considerable pressure range it offers and the clearly defined stretch rate $K = (2/R_f)\dot{R}_f$, where R_f and $\dot{R}_f$ denote the flame radius and the flame displacement speed in the laboratory frame, respectively [3]. The relatively low laminar flame speed of ammonia leads to long time scales in experiments. As the flame expands, radiation and buoyancy become increasingly important. These challenges can be avoided by increasing the oxygen content in the oxidizer [4,5] or by blending ammonia with faster-burning energy carriers such as hydrogen [6,7] and methane [8] to accelerate the flame. The major disadvantage of these methods is that they alter the chemistry of the investigated flames, changing flame temperatures and structure. To fully understand ammonia combustion at low reactivity conditions, the elimination of both buoyancy and radiation-induced uncertainties is required. Thus, high-fidelity ammonia/air flame speed data are of great interest.

The radiation-induced $S^0_{L,u}$ reduction of OPFs can be estimated using the radiation correction formula proposed by Yu et al. [9]. This formula

* Corresponding author.
E-mail address: r.glaznev@itv.rwth-aachen.de (R. Glaznev).

https://doi.org/10.1016/j.proci.2024.105334
Received 5 December 2023; Accepted 4 June 2024

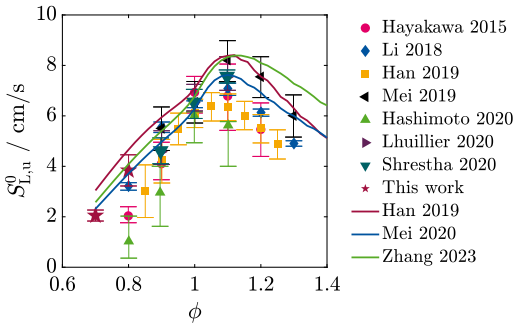

Fig. 1. Unstretched laminar flame speed $S^0_{L,u}$ vs. fuel–air equivalence ratio ϕ for ammonia/air flames ($p_{u,0} \approx 1$ atm, $T_{u,0} \approx 298$ K) without radiation correction. Points denote experiments: [4,6–8,11,12,14], lines - simulations using mechanisms [16–18].

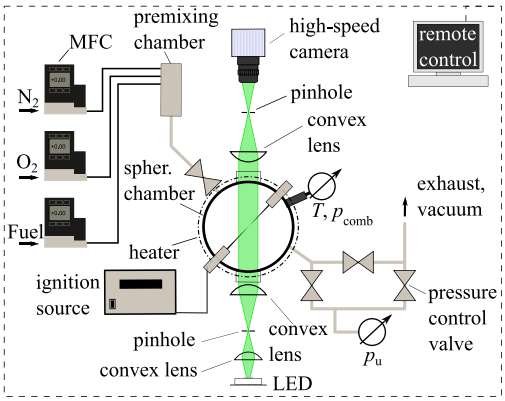

Fig. 2. Schematic of the microgravity experimental setup.

was validated against numerical simulations of methane and iso-octane OPFs with $S^0_{L,u} > 9$ cm/s using the statistical narrow-band model (SNB). Recently Faghih et al. [10] conducted a complementary numerical analysis for ammonia flames with $S^0_{L,u} > 4$ cm/s using the optically thin radiation model (OTM). The authors concluded that the updated formula by Faghih et al. should be applied for radiation correction of the experimental ammonia flames with $S^0_{L,u} < 9$ cm/s instead of the formula by Yu et al. However, the formulas have not been validated against experimental $S^0_{L,u} < 4$ cm/s.

Additionally to radiation, slowly-burning flames can be affected by buoyancy, which strongly deforms the flame and influences the accuracy of the flame speed determination. There are several approaches to identify the buoyancy-affected stage of flame propagation. Hayakawa et al. [11] investigated ammonia/air $S^0_{L,u}$ up to unburned gas pressure $p_{u,0} = 5$ bar. They tracked the ratio of vertical to horizontal radius and checked the flame propagation speed consistency to identify the buoyancy-unaffected flame propagation stage. This method decreased the maximum processed R_f to 1.5 cm for fuel–air equivalence ratio $\phi = 1$, leading to increased stretch extrapolation uncertainties, meaning even stricter R_f restrictions and higher uncertainties for slower flames. A similar approach was applied by Hashimoto et al. [12] for ammonia and ammonia/methane blends. Pfahl et al. [13] and Li et al. [14] used horizontal radius to minimize buoyancy-induced uncertainty. Mei et al. [4] used the same method for ammonia/air flames with increased oxygen content. However, a recent DNS study by Berger et al. [15] has shown that this radius extraction method is prone to significant errors.

The buoyancy effect can be eliminated experimentally using microgravity facilities like drop towers [19]. Microgravity experiments are, however, complicated and, as a result, rare. One of the primary objectives of the current study is to isolate the radiation-induced uncertainty by conducting high-fidelity experiments in microgravity. There is no data on ammonia flame propagation in microgravity, except the work by Ronney et al. [20] from 1988, where the dependence of $\dot{R}_f$ on stretch rate was neglected. Therefore, experimental uncertainties caused by radiation and buoyancy effects must be analyzed and understood.

Fig. 1 presents a data comparison between the latest experimental ammonia/air $S^0_{L,u}$ obtained at normal conditions without a radiation correction model and adiabatic planar flame simulations. The equivalent figures with the experimental results corrected using the formulas by Yu et al. and Faghih et al. are presented in Supplementary materials in Fig. S1. Significant scatter is observed even for the data since 2015 obtained using modern data acquisition techniques. Especially large difference can be seen for $\phi < 0.9$ and $\phi > 1.1$, closer to the flame propagation limits. Since the flame speeds in these ranges are even slower and more strongly affected by buoyancy and radiation, which are complicated to consider accurately in simulations, it is important to minimize their effect on experimental results. Furthermore, it is not clear how these uncertainties can affect the analysis of the performance of the chemical kinetic models.

With these highlighted challenges, the present study deals with the following questions:

1. How do radiation correction methods by Yu and Faghih perform for experimental $S^0_{L,u} < 4$ cm/s?
2. How well do existing kinetic models predict ammonia flame speeds near propagation limits?
3. How significantly can radiation correction change kinetic model assessment?

2. Experimental framework

2.1. Apparatus and procedures

The experimental setup and post-processing procedures used in this study are similar to those in the work by Hesse et al. [19], so only a brief introduction is presented here. Microgravity experiments were conducted in ZARM's (Center of Applied Space Technology and Microgravity) prototype high-repetition drop tower facility called the GraviTower Bremen Prototype (GTB Pro) providing up to 2.5 s with less than 10^{-4} g during drops.

The experimental setup, schematically illustrated in Fig. 2, includes a spherical combustion chamber with an inner diameter of 100.5 mm. The vertically-installed Schlieren arrangement consists of a dual-field lens configuration in the center, a CMOS camera at the top, and a high-power LED at the bottom. Flame images with a size of 800×832 pixels were recorded at 10000 frames per second (fps), providing a spatial resolution of 17.32 pixel/mm.

The mixture preparation process is controlled remotely with solenoid valves, mass flow controllers, and a pressure-regulating valve at the chamber outlet. Details about mixture preparation uncertainty are given in the Supplementary material. A two-step coil and capacitor ignition system provides spark energies up to 5 J. Sparks are discharged through two elongated tapering spark plug electrodes positioned opposite each other with tip diameters of 0.3 mm and the gap between electrode tips of 1.3 mm.

Each experiment was repeated 2–3 times with varying ignition energy minimizing ignition effects and identifying the ignition affected (I), transitioning (II), and self-sustainable (III) regimes of flame propagation (Fig. 3).

A high-accuracy Keller 35XHTC and a high-frequency Kistler 4011 A pressure transducers were used to measure pressure before and during combustion, respectively. Pressure data were recorded at 10000 Hz. The combustion chamber can be heated for measurements at elevated temperatures.

In the present study, ammonia/air flame propagation was investigated under microgravity (μg) in three sets of cases (cf. Table 1). Case

Table 1
Overview of the selected initial conditions, maximum pressures, and temperatures for $S^0_{L,u}$ extraction.

Case #	$p_{u,0}$ bar	$T_{u,0}$ K	p^{max} bar	T^{max} K	ϕ –
C1	1.013	298	>2.5	>381	0.7, 0.8, 1.3
C2	1.5	332	>4	>433	0.7, 0.8, 1.3
C3	3	373	>8	>484	0.7, 1.3

C2 is designed to have initial unburned gas pressure $p_{u,0}$ and temperature $T_{u,0}$ on the isentrope of C1, leading to overlapping and cross-validating flame speed data obtained using the pressure-rise method. The C3 case is designed to reach a higher pressure–temperature combination, which has never been studied before near the flame propagation limits.

2.2. Flame speed extraction from optical data

Flame front extraction is limited to spherical smooth flame fronts above a critical radius associated with the complete decay of ignition artifacts and within a quasi-isobaric regime. The background is removed from Schlieren images, and the flame front is obtained using the method by Otsu et al. [21]. This provides the temporal evolution of the flame radius $R_f(t)$ at its iso-temperature surface of approximately 850 K [22]. Central differences are applied to obtain the stretched propagation speed of a burned mixture $S_{L,b} = \dot{R}_f = dR_f/dt$ assuming motionless burned gas. Stretch rate K is defined as the temporal change of the flame surface area A_f, which for OPF is $K = 1/A_f \cdot dA_f/dt = 2/R_f \cdot dR_f/dt$. The nonlinear expression by Kelley et al. [23] is used to extrapolate the flame speed to zero stretch $S^0_{L,b}$ (denoted with the superscript "0") and the Markstein length $\mathcal{L}_b$. The unstretched laminar flame speed of the unburned gas, $S^0_{L,u}$, can be evaluated for adiabatic flames assuming mass continuity through a planar unstretched flame, $S^0_{L,u} = S^0_{L,b}(\rho_b/\rho_u)$, where ρ_b and ρ_u are the burned and unburned densities determined in 0D equilibrium calculations. A slowly-burning flame can render this relation and the motionless burned gas assumption invalid due to radiation heat loss, as discussed by Hesse et al. [24]. In the present study, the approaches by Yu et al. [9] and Faghih et al. [10] are used for radiation correction.

2.3. Flame speed extraction from pressure- rise data

Several assumptions are invoked to calculate $S_{L,u}$ from pressure data, including infinitely thin smooth spherical flame fronts during combustion, spatially uniform pressure during combustion, isentropic compression, ideal combustion of both burned and unburned gases, and negligible radiation and buoyancy effects. This method and its errors in fast-burning flames using a two-zone model were recently discussed in Bariki et al. [25]. For slow-burning flames, as investigated by Hesse et al. [19], a multi-zone model, such as the Mass- and Energy-Conserving Thermo (MECT) introduced by Elia et al. [26], is required to correct for radiation heat losses. This improves the depiction of the burned gas temperature decrease.

Here, we selected the National Institute of Standards and Technology's (NIST) data reduction tool for spherical constant volume flame experiments [27], which uses the MECT multi-zone model. The pressure data were processed by applying a moving average scheme. The stretch effect was minimized by using $p/p_0 > 2$, where p_0 is the initial chamber pressure. This limit was analyzed earlier by Halter et al. [28]. Here, the stretch rate derived from pressure data typically fell within the range of 3 to 12 s^{-1} with $R_f > 3.9$ cm, which is smaller than the characteristic stretch rates observed using the optical method (Fig. S2). Therefore, the stretch effect is considered negligible in the extracted press-rise data. The wall heat loss effect was minimized by evaluating pressure rise until the pressure inflection point given by its maximum second order time derivative max($\ddot{p}$).

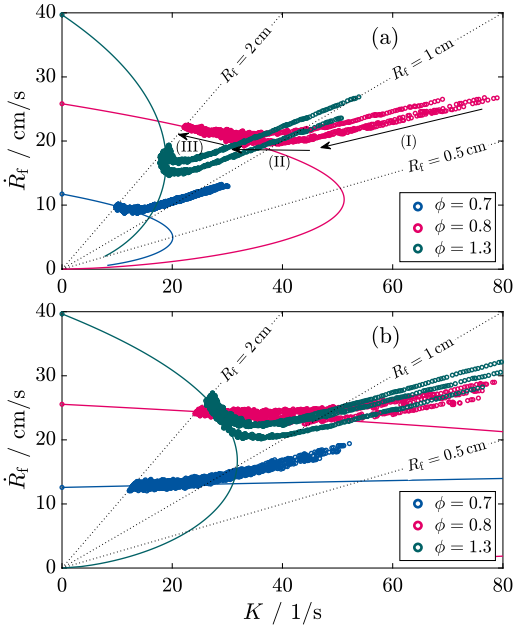

Fig. 3. Flame propagation speed dependence on stretch rate for (a) C1: $p_{u,0} = 1.013$ bar, $T_{u,0} = 298$ K; and (b) C2: $p_{u,0} = 1.5$ bar, $T_{u,0} = 332$ K. Points represent measured values, lines - characteristic extrapolation.

Radiation emission was modeled for species in the burned equilibrated gas for H_2O, NO, N_2O, and NH_3 as major radiative components using the optically thin model (OTM), thus neglecting radiation absorption. Planck-mean absorption coefficients of NO, N_2O, and NH_3 were taken from [10,29]. The combined uncertainty of the pressure-rise method does not exceed ±6% of $S^0_{L,u}$. Handling radiation in the pressure-rise method in a statistical narrow-band model framework is out of the scope of this work, meaning that radiation correction can be overestimated. Zheng et al. [30] investigated radiation reabsorption in planar ammonia/hydrogen flames. They found a 15.6%-increase of $S^0_{L,u}$ due to radiation reabsorption in comparison with the results obtained using optically thin model (OTM). However, a similar analysis has not yet been conducted for spherically expanding ammonia flames, which are expected to have lower optical thickness and to be affected less by reabsorption [10].

3. Numerical framework

One-dimensional simulations of stationary unstretched flames were performed using the appropriate modules of the open-source program FlameMaster [31]. Gradients are properly resolved using a dynamic grid refinement algorithm. At least 200 grid points resolve the reaction zone.

Ammonia/air flames are modeled using three recently developed chemical kinetic model by Mei et al. [17], Han et al. [16], and Zhang et al. [18]. The models were selected based on the recent work by Girhe et al. [32], who conducted a comprehensive kinetic model evaluation, considering 16 recent models based on their quantitative performance in predicting literature data on NH_3/H_2 combustion. The chosen kinetic models exhibit the overall best performance predicting laminar flame speed data reported in 12 recent studies, making them promising for comparison near the propagation limits. All simulations are conducted assuming no gas radiation for comparison with the radiation-corrected experimental data.

4. Results and discussion

4.1. Stretch dependence in ammonia/air flames

The dependence of the flame propagation speed on the stretch rate is presented in Fig. 3 for C1 and C2. For C1 with $p_{u,0} = 1.013$ bar, positive Markstein lengths are observed for $\phi = 0.7$ and 0.8. Flames at $\phi = 1.3$ were found to have strong nonlinear dependence on stretch with highly positive Markstein length. This behavior leads to substantially higher extrapolated $S^0_{L,b}$ and $S^0_{L,u}$ values than those for $\phi = 0.7$ and 0.8, even though local $\dot{R}_f$ are of similar order of magnitude. Therefore, all the flames of $\phi = 0.7$, 0.8, and 1.3 have similar experimental timescales and are buoyant under normal gravity. Strong nonlinear stretch dependence together with highly positive Markstein length significantly decreased the data range available for extrapolation and increased extrapolation-related uncertainty for $\phi = 1.3$. Therefore, optical data of $\phi = 1.3$ at $p_{u,0} = 1.013$ bar was not considered in further analysis.

With $p_{u,0}$ and $T_{u,0}$ increased to 1.5 bar and 332 K, respectively, the $\dot{R}_f$ dependence on the stretch rate changes (Fig. 3, b). The Markstein length for the $\phi = 0.7$ flames becomes slightly negative, potentially leading to instabilities at higher pressures. The $\dot{R}_f$ dependence on the stretch rate for $\phi = 1.3$ flames is weaker, but the Markstein length stays positive. It widens the data available range for extrapolation relatively to the one at 1.013 bar, allowing $S^0_{L,u}$ extraction using the optical method. Illustrative is that this minor change in $p_{u,0}$ and $T_{u,0}$ is sufficient to change the $\dot{R}_f$ response on the stretch rate, but does not change significantly extrapolated $S^0_{L,b}$ and $S^0_{L,u}$ values.

It is worth noting that the Markstein length for $\phi = 0.7$ is positive at $p_{u,0} = 1.013$ bar for the investigated mixtures with normal air (Fig. 3, a), while in [33] the Markstein length is negative for ammonia/pure oxygen mixtures with $\phi = 0.7$, making it sensitive to the oxygen content in the oxidizer. Thus, the observed stretch behavior of ammonia/air flames would not be captured if buoyancy was suppressed by increased O_2 content.

4.2. Flame speeds from pressure-rise method

Flame speeds extracted using the pressure-rise method during near-isentropic compression of the unburned gas at $\phi = 0.8$ for C1 and C2 are presented in Fig. 4. Top and bottom abscissas represent the isentropic increase of pressure and unburned gas temperature. Dotted lines represent $S^0_{L,u}$ obtained by planar flame simulations. Dashed lines correspond to the power-law fit (Eq. S1) of the experimental data depicted with solid lines. The power-law fit parameters are presented in Table S1.

Flames from C1 and C2 cases are expected to expand according to the same isentrope. Consequently, flame speeds extracted from these cases using the pressure-rise method should overlap with each other if the flame stretch and flame–wall interaction affected pressure-rise signal is properly excluded from the post-processing. As one can see in Fig. 4, these two data sets represent a consistent progression, highlighting the accuracy of the conducted experiments and applied post-processing routine. The same consistency can be observed for $\phi = 0.7$ and 1.3 in Fig. 5.

Radiation correction of the flame speeds extracted using the pressure-rise method changes the perception of the best-performing mechanism significantly. First, at $p_u = 2$ bar, uncorrected data lies between the simulation results obtained using the kinetic models of Zhang et al. and Mei et al. Then, with p_u rising up to 4.5 bar, experimental $S_{L,u}$ lies on the Mei et al. simulations. With that, one could conclude that the model by Mei et al. is the best one for ammonia/air lean flame speed prediction at $p_u < 4.5$ bar.

However, the situation is changing once radiation correction is applied. Now, at $p_u = 2$ bar, the corrected experimental results lie between the simulation results with the models by Han et al. and Zhang et al.

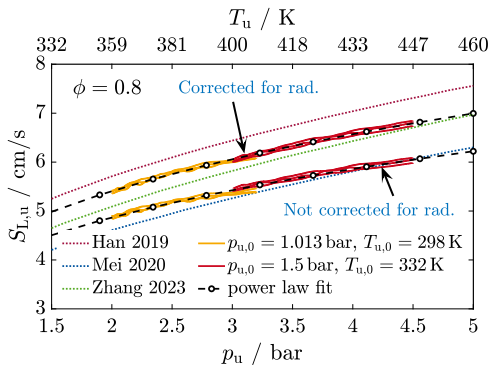

Fig. 4. Flame speed with and without radiation correction during the near-isentropic unburned gas compression at $\phi = 0.8$ for C1: $p_{u,0} = 1.013$ bar, $T_{u,0} = 298$ K, and C2: $p_{u,0} = 1.5$ bar, $T_{u,0} = 332$ K. Solid lines - experiments, dashed lines - fit, dotted lines - simulations.

while the model by Mei et al. significantly underpredicts $S_{L,u}$. When p_u increases up to 4.5 bar, the flame speed simulated using the Zhang et al. model has a much better agreement with the experimental results, with Han et al. and Mei et al. overpredicting and underpredicting experiments, respectively.

Thus, combining high-fidelity data over a wide pressure and temperature range with carefully carried out radiation correction allows us to evaluate chemical kinetic model performance properly. For this reason, hereafter pressure-rise data are presented only with the radiation correction applied.

An overview of the measured flame speed over a wide range of p_u and T_u for all the studied cases is presented in Fig. 5. All the optical results are corrected for radiation using the formula by Yu et al. [9]. Additionally, optical results for $p_u = 1.013$ bar, $T_u = 298$ K are corrected by the Faghih et al. formula [10]. A good agreement between the radiation-corrected pressure-rise data and the Yu-corrected optical data is observed for all the investigated cases. This cross-validation of the optical and pressure method results, data for which were captured using independent experimental devices, allows a conclusion on the fidelity of the obtained data. Observed overprediction of the radiation correction by the Faghih formula at $p_u = 1$ atm, $T_u = 298$ K can be caused either by the fact that this formula was not validated against $S^0_{L,u} < 4$ cm/s, or that Faghih et al. used an extrapolation range of $2 < R_f < 3$ cm, when in the current work only data until $R_f < 2$ cm are available. It is worth noting that the differences in model predictions in Fig. 4 and Fig. 5 are comparable to the radiation effect, reflecting the inherent substantial uncertainties of the kinetic parameters within the ammonia kinetic models.

4.3. Radiation effect on evaluation of kinetic model performance

Quantification of the chemical kinetic models' performances with respect to the obtained experimental datasets is required for understanding how the radiation correction affects kinetic model assessment. Here, the pressure-rise method flame speed results were chosen for evaluation since they provide laminar flame speed data in much wider ranges of the unburned gas temperatures (< 500 K) and pressures (< 9.3 bar) than the optical method.

The agreement between the model predictions and the experimental data was quantified using the curve similarity index, referred to as curve matching score [34]. This score, which varies from 0 to 1, reflects the level of similarity between two curves, considering not only the absolute differences but also their correlation and the similarity of their first derivatives. A score of 1 denotes perfect alignment. Here, assessments were conducted using the SciExpeM framework [35].

Table 2 represents scores describing the agreement between the models' predictions against the original and radiation-corrected laminar

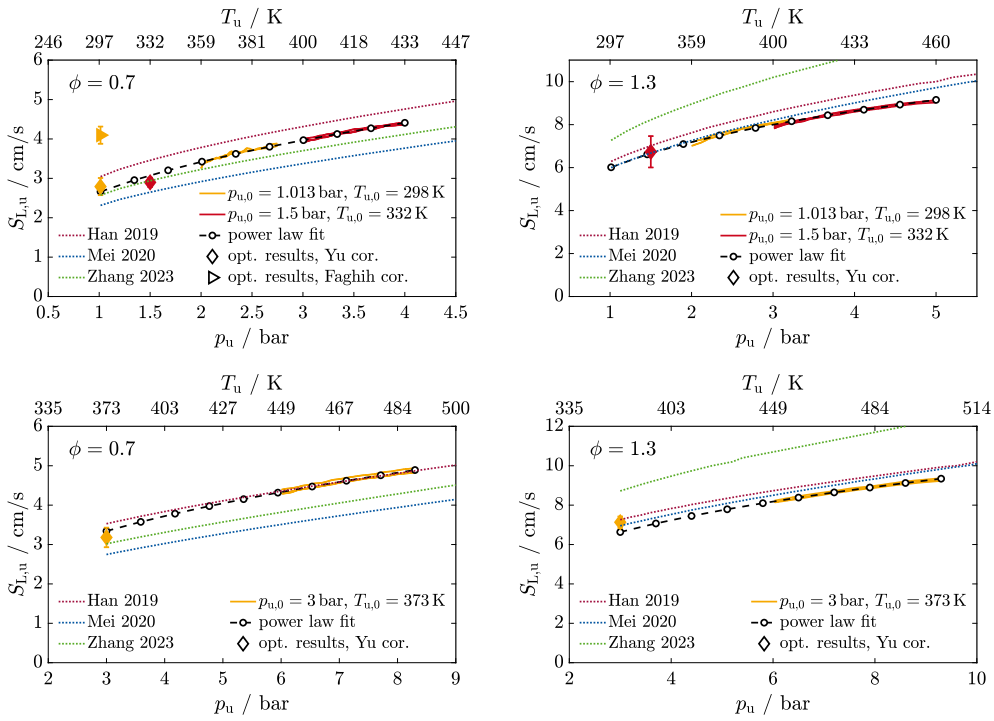

Fig. 5. Flame speed dependence on pressure and temperature for varying equivalence ratio and initial p_u and T_u. Closed symbols denote optical method results (diamonds - corrected for rad. by Yu et al.'s [9] formula, triangles - corrected for rad. by Faghih et al.'s [10] formula), solid lines - pressure method results, dotted lines - simulation results.

Table 2
Comparison of curve matching scores of the chemical kinetic models. The score values in the first and the second columns under each ϕ represent model prediction agreement without and with radiation correction, respectively. The color scale from green to red indicates the descending prediction accuracy of each dataset for each ϕ.

Kinetic model	$p_u < 5$ bar, $T_u < 460$ K						$p_u > 5$ bar, $T_u > 427$ K				Mean	
	$\phi = 0.7$		$\phi = 0.8$		$\phi = 1.3$		$\phi = 0.7$		$\phi = 1.3$			
	No rad. c.	Rad. cor.	No rad. c.	Rad. cor.	No rad. c.	Rad. cor.	No rad. c.	Rad. cor.	No rad. c.	Rad. cor.	No rad. c.	Rad. cor.
Han 2019	0.549	0.633	0.628	0.700	0.717	0.795	0.689	0.932	0.724	0.847	0.670	0.802
Mei 2020	0.714	0.401	0.714	0.464	0.740	0.839	0.713	0.591	0.732	0.865	0.725	0.674
Zhang 2023	0.628	0.565	0.695	0.696	0.647	0.690	0.794	0.642	0.646	0.720	0.679	0.654

flame speed datasets across different pressures and equivalence ratios. Each set of conditions is represented by two columns: the left column shows scores for the original uncorrected data and the right column for the radiation-corrected data.

For $p_u < 5$ bar, the Mei model showed the best agreement with the original data under lean conditions, followed by the Zhang and the Han model. However, a contrasting evaluation arises when comparing the models to the radiation-corrected data. Now, rather than being the least favorable among the three analyzed models, the model by Han exhibits the highest concordance with the experiment at $\phi = 0.7$, outperforming the Mei and Zhang models by approximately $\sim$ 33 % and $\sim$ 6 %, respectively. It is worth mentioning that scores of the Han and Zhang models become comparable at $\phi = 0.8$, highlighting that the performance analysis of these mechanisms at other equivalence ratios and mixture conditions is required. Similar performance is observed at $\phi = 0.7$ for $p > 5$ bar, where the score of the Han model significantly improved after the radiation correction, becoming $\sim$ 33 % and $\sim$ 31 % better than the Mei and Zhang models, respectively.

At rich conditions, all models showed significant overprediction of the experimental data without radiation correction for all investigated pressures. For this reason, the introduction of the radiation correction did not affect the models' relative ranking but significantly improved all the scores.

The mean score highlights that the Han model performs best in predicting the radiation-corrected experimental flame speed data despite having the lowest average score for the uncorrected data. The Mei model showed moderate mean scores stemming from its best and worst prediction agreement against the data at rich and lean conditions, respectively.

The Zhang model exhibited the lowest scores, especially because of its overprediction under rich conditions. The radiation correction, which increases measured flame speeds, led to reduced overpredictions with the original data, as reflected in the improved scores. However, a decrease in mean scores with radiation correction was observed, attributed to increased underpredictions in lean conditions. This assessment indicates the need for further refinement of the Zhang model, considering its otherwise robust predictive capabilities across a broad range of conditions [36]. Ammonia flame speed, particularly in the local fuel-rich areas, is sensitive to the pyrolysis reactions in the flame zone alongside the oxidation chemistry [37]. The discrepancies in the model performance may be linked to significant uncertainties in the NH_3 pyrolysis mechanism, primarily due to complex radical–radical reactions that pose challenges in their characterization [37].

5. Concluding remarks

In the present study, the role of the radiation effect on ammonia/air flame speeds near the propagation limits was examined under microgravity using the optical and pressure-rise methods simultaneously. The main outcomes of the present study are summarized as follows:

- High-fidelity experiments were conducted with slowly propagating ammonia/air mixtures under microgravity to isolate the radiation effect from buoyancy
- The flame speed's dependence on stretch was analyzed under near-isobaric conditions using the optical method. It was shown that for $\phi = 1.3$ strong nonlinear stretch response of flame propagation speed is observed up to $R_f = 2$ cm, which was significantly decreased at $p_{u,0} = 1.5$ bar, $T_{u,0} = 332$ K.
- Flame speed data extracted using the pressure-rise during near-isentropic gas compression were analyzed. Overlapping results obtained from two datasets along the same isentrope showed a consistent progression for all the investigated equivalence ratios, highlighting high fidelity of the conducted experiments.
- Flame speed data were analyzed with respect to the response to the radiation correction. It was found that optical data corrected for radiation using the formula by Yu et al. show good agreement with the radiation-corrected pressure-rise data, thus cross-validating the two methods applied.
- For the first time, chemical kinetic models' assessment over a wide pressure and temperature range was conducted for very low ammonia flame speeds close to flame propagation limits. Kinetic models' performance with respect to the radiation-corrected and non-corrected flame speed data was quantified using the curve similarity index.
- Significant dependence of the kinetic model performance score of the radiation correction presence was observed. For $\phi = 1.3$, the radiation correction did not change the ranking order of the kinetic models, but significantly improved the scores. For $\phi = 0.7$ and 0.8, radiation correction of the experimental data resulted in changes in the chemical kinetic model ranking, highlighting the necessity of radiation correction for further experimental investigation of ammonia/air flame speeds.

Novelty and significance statement

Obtaining ammonia flame speed data for very low flame speeds is extremely challenging. The novelty of this research is a combination of two experimental techniques applied simultaneously to obtain unique high-fidelity ammonia/air slowly propagating flame speed data under microgravity. Both techniques rely on different principles and cross-validate each other at various conditions. Measurements are further processed with radiation correction schemes to carefully quantify their combined influence on chemical kinetic model assessment in a wide range of unburned gas temperatures (< 500 K) and pressures (< 9.3 bar). This study underscores the significance of precise radiation correction, as its improper handling can yield erroneous assessments of ammonia kinetic model performance, thereby holding considerable relevance for the scientific community.

CRediT authorship contribution statement

Roman Glaznev: Conceptualization, Experiments, Simulations, Writing – original draft. **Christian Schwenzer:** Experiments, Consultation, Writing – review & editing. **Raik Hesse:** Experiments, Consultation, Writing – review & editing. **Sanket Girhe:** Consultation, Writing – review & editing. **Fabien Halter:** Consultation, Writing – review & editing. **Christian Chauveau:** Consultation, Writing – review & editing. **Heinz Pitsch:** Supervision, Writing – review & editing. **Joachim Beeckmann:** Supervision, Writing – review & editing.

Declaration of competing interest

The authors declare that they have no known competing financial interests or personal relationships that could have appeared to influence the work reported in this paper.

Acknowledgments

The authors gratefully acknowledge the generous support of Deutsche Forschungsgemeinschaft (DFG, German Research Foundation, Germany, Grant No. 469834263 , Cluster of Excellence 2186 "The Fuel Science Center", Grant No. 390919832) and Deutsches Zentrum fur Luft- und Raumfahrt (DLR, German Aerospace Center, Grant No. 50WM2258). We thank the European Space Agency (ESA) for funding and the Center of Applied Space Technology and Microgravity (ZARM), Germany for providing the drops in the GraviTower Bremen Pro.

Appendix A. Supplementary data

Supplementary material related to this article can be found online at https://doi.org/10.1016/j.proci.2024.105334.

References

[1] A. Valera-Medina, H. Xiao, M. Owen-Jones, W. David, P. Bowen, Ammonia for power, Prog. Energ. Combust. 69 (2018) 63–102.
[2] Solutions, MAN Energy, MAN B&W two-stroke engine operating on ammonia, 2021.
[3] S.M. Candel, T.J. Poinsot, Flame stretch and the balance equation for the flame area, Combust. Sci. Technol. 70 (1–3) (1990) 1–15.
[4] B. Mei, X. Zhang, S. Ma, M. Cui, H. Guo, Z. Cao, Y. Li, Experimental and kinetic modeling investigation on the laminar flame propagation of ammonia under oxygen enrichment and elevated pressure conditions, Combust. Flame 210 (2019) 236–246.
[5] A. Karan, G. Dayma, C. Chauveau, F. Halter, Experimental study and numerical validation of oxy-ammonia combustion at elevated temperatures and pressures, Combust. Flame 236 (2022).
[6] K.P. Shrestha, C. Lhuillier, A.A. Barbosa, P. Brequigny, F. Contino, C. Mounaïm-Rousselle, L. Seidel, F. Mauss, An experimental and modeling study of ammonia with enriched oxygen content and ammonia/hydrogen laminar flame speed at elevated pressure and temperature, Proc. Combust. Inst. (2020).
[7] C. Lhuillier, P. Brequigny, F. Contino, C. Mounaïm-Rousselle, Experimental study on ammonia/hydrogen/air combustion in spark ignition engine conditions, Fuel 269 (2020) 117448.
[8] X. Han, Z. Wang, M. Costa, Z. Sun, Y. He, K. Cen, Experimental and kinetic modeling study of laminar burning velocities of NH_3/air, NH_3/H_2/air, NH_3/CO/air and NH_3/CH_4/air premixed flames, Combust. Flame 206 (2019) 214–226.
[9] H. Yu, W. Han, J. Santner, X. Gou, C. Sohn, Y. Ju, Z. Chen, Radiation-induced uncertainty in laminar flame speed measured from propagating spherical flames, Combust. Flame 161 (11) (2014) 2815–2824.
[10] M. Faghih, A. Valera-Medina, Z. Chen, A. Paykani, Effect of radiation on laminar flame speed determination in spherically propagating NH_3-air, NH_3/CH_4-air and NH_3/H_2-air flames at normal temperature and pressure, Combust. Flame 257 (2023) 113030.
[11] A. Hayakawa, T. Goto, R. Mimoto, Y. Arakawa, T. Kudo, H. Kobayashi, Laminar burning velocity and Markstein length of ammonia/air premixed flames at various pressures, Fuel 159 (2015) 98–106.
[12] G. Hashimoto, K. Hadi, Y. Xia, A. Hamid, N. Hashimoto, A. Hayakawa, H. Kobayashi, O. Fujita, Turbulent flame propagation limits of ammonia/methane/air premixed mixture in a constant volume vessel, Proc. Combust. Inst. (2020).
[13] U. Pfahl, M. Ross, J. Shepherd, K. Pasamehmetoglu, C. Unal, Flammability limits, ignition energy, and flame speeds in H2–CH4–NH3–N2O–O2–N2 mixtures, Combust. Flame 123 (1) (2000) 140–158.
[14] Y. Li, M. Bi, B. Li, W. Gao, Explosion behaviors of ammonia–air mixtures, Combust. Sci. Technol. 190 (10) (2018) 1804–1816.
[15] L. Berger, R. Hesse, K. Kleinheinz, M.J. Hegetschweiler, A. Attili, J. Beeckmann, G.T. Linteris, H. Pitsch, A DNS study of the impact of gravity on spherically expanding laminar premixed flames, Combust. Flame 216 (2020) 412–425.
[16] X. Han, Z. Wang, M. Costa, Z. Sun, Y. He, K. Cen, Experimental and kinetic modeling study of laminar burning velocities of NH_3/air, NH_3/H_2/air, NH_3/CO/air and NH_3/CH_4/air premixed flames, Combust. Flame 206 (2019) 214–226.
[17] B. Mei, S. Ma, Y. Zhang, X. Zhang, W. Li, Y. Li, Exploration on laminar flame propagation of ammonia and syngas mixtures up to 10 atm, Combust. Flame 220 (2020) 368–377.
[18] X. Zhang, K.K. Yalamanchi, S. Mani Sarathy, Combustion chemistry of ammonia/C1 fuels: A comprehensive kinetic modeling study, Fuel 341 (2023) 127676.
[19] R. Hesse, C. Bariki, M.J. Hegetschweiler, G.T. Linteris, H. Pitsch, J. Beeckmann, Elucidating the challenges in extracting ultra-slow flame speeds in a closed vessel—A CH_2F_2 microgravity case study using optical and pressure-rise data, Proc. Combust. Inst. (2022).

[20] P. Ronney, Effect of chemistry and transport properties on near-limit flames at microgravity, Combust. Sci. Technol. 59 (1–3) (1988) 123–141.
[21] N. Otsu, A threshold selection method from gray-level histograms, IEEE Trans. Syst. Man Cybern. 9 (1) (1979) 62–66.
[22] D. Dunn-Rankin, F. Weinberg, Location of the schlieren image in premixed flames: Axially symmetrical refractive index fields, Combust. Flame (1998).
[23] A. Kelley, J. Bechtold, C. Law, Premixed flame propagation in a confining vessel with weak pressure rise, J. Fluid Mech. 691 (2012) 26–51.
[24] R. Hesse, L. Berger, C. Bariki, M.J. Hegetschweiler, G.T. Linteris, H. Pitsch, J. Beeckmann, Low global-warming-potential refrigerant CH_2F_2 (R-32): Integration of a radiation heat loss correction method to accurately determine experimental flame speed metrics, Proc. Combust. Inst. 38 (3) (2021) 4665–4672.
[25] C. Bariki, R. Hesse, F. Halter, H. Pitsch, J. Beeckmann, Combined isochoric and isobaric acquisition methodology for accurate flame speed measurements from ambient to high pressures and temperatures, Proc. Combust. Inst. 38 (2) (2021) 2185–2193.
[26] M. Elia, M. Ulinski, M. Metghalchi, Laminar Burning Velocity of Methane–Air–Diluent Mixtures, J. Eng. Gas Turbines Power 123 (1) (2000) 190–196.
[27] M. Hegetschweiler, G.T. Linteris, Data reduction tool for spherical constant volume flame experiments, 2021, http://dx.doi.org/10.6028/NIST.TN.2148, NIST Technical Note 2148 Gaithersburg.
[28] F. Halter, G. Dayma, Z. Serinyel, P. Dagaut, C. Chauveau, Laminar flame speed determination at high pressure and temperature conditions for kinetic schemes assessment, Proc. Combust. Inst. (2020).
[29] H. Nakamura, M. Shindo, Effects of radiation heat loss on laminar premixed ammonia/air flames, Proc. Combust. Inst. 37 (2) (2019) 1741–1748.
[30] S. Zheng, H. Liu, R. Sui, B. Zhou, Q. Lu, Effects of radiation reabsorption on laminar NH_3/H_2/air flames, Combust. Flame 235 (2022) 111699.
[31] H. Pitsch, FlameMaster: A C++ computer program for 0D combustion and 1D laminar flame calculations, 1998.
[32] S. Girhe, A. Snackers, T. Lehmann, R. Langer, F. Loffredo, R. Glaznev, J. Beeckmann, H. Pitsch, Ammonia and ammonia/hydrogen combustion: Comprehensive quantitative assessment of kinetic models and examination of critical parameters, Combust. Flame 267 (2024) 113560.
[33] Q. Liu, X. Chen, J. Huang, Y. Shen, Y. Zhang, Z. Liu, The characteristics of flame propagation in ammonia/oxygen mixtures, J. Hazard. Mater. 363 (2019) 187–196.
[34] E. Ramalli, T. Dinelli, A. Nobili, A. Stagni, B. Pernici, T. Faravelli, Automatic validation and analysis of predictive models by means of big data and data science, Chem. Eng. J. 454 (2023) 140149.
[35] SciExpeM, 2023 (Accessed on 01 March 2023).
[36] A.G. Szanthoffer, I.G. Zsély, L. Kawka, M. Papp, T. Turányi, Testing of NH_3/H_2 and NH_3/syngas combustion mechanisms using a large amount of experimental data, Appl. Energy Combust. Sci. 14 (2023) 100127.
[37] P. Glarborg, H. Hashemi, P. Marshall, Challenges in Kinetic modeling of ammonia pyrolysis, Fuel Comm. 10 (2022) 100049.